Appendix B

UV Imaging of the Galaxy Cluster Abell 851 at z=0.41[1]

Abstract

The first UV F300W and F218W WFPC2 observations of the rich galaxy cluster CL0939+4713 at z = 0.41 are presented and discussed. UV/optical two-color and c-m diagrams of the sources detected in the F300W waveband are constructed. Thanks to pre-existing HST optical images of the same field a morphological classification for the majority of these objects is also provided. Moreover, taking advantage of recent redshift surveys along CL0939+4713 line of sight, separate diagrams comparing the properties of galaxies belonging to the cluster and to its close projected field are presented. Possible evolutionary effects in the UV from z ∼0.4 to present time are investigated by comparing the restframe [mid-UV−Optical] colors of galaxies in CL0939+4713 with balloon-borne data of the Coma cluster, as well as by resorting to suitable galaxy evolution models. Finally, current attempts to constrain the epoch of the UV-upturn onset in evolved populations by means of HST UV observations are discussed.

B.1 Introduction

Owing to its high richness and distance (z=0.41), CL0939+4713 = Abell 851 turns out to be one of the "most wanted" targets both for morphological and evolutionary studies of galaxy clusters, thus being presently one of the best known intermediate-redshift systems. Extensive analyses, including both imaging and spectroscopy, have been carried out from ground in the optical (Dressler & Gunn 1983; 1992; Fukugita *et al.* 1995; Belloni *et al.* 1995; Belloni & Röser 1996; Dressler *et al.* 1999) and in the IR (Stanford *et al.* 1995, 1998). Besides the above ground-based studies, a large amount of space-borne (HST, ROSAT) observing time has been devoted to survey this cluster (Dressler *et al.* 1994a, 1994b, 1997; Seitz *et al.* 1996; Oemler *et al.* 1997; Smail *et al.* 1997; Andreon *et al.* 1997; Schindler & Wambsganss 1996; Schindler *et al.* 1998).

An important outcome of such – mainly optical – observational effort is the identification in CL0939+4713 (as well as in the cores of other rich clusters of comparable redshift) of a larger fraction of star-forming galaxies. Such a phenomenon, commonly referred to as the

[1]Buson, L. M., Bertola, F., Cappellari, M., Chiosi, C., Dressler, A. & Oemler, A. J. 2000, ApJ, 531, 684

Butcher–Oemler effect (Butcher & Oemler 1978; 1984), is related, in turn, to an excess of late–type spirals, irregulars and mergers, when compared with the nearby cluster galaxy population (e.g. Couch *et al.* 1994, 1998; Oemler *et al.* 1997). Analogously, a remarkably higher proportion of the post-star-forming a+k and/or k+a galaxies (previously termed a bit improperly E+A galaxies) can be recognized in these intermediate redshift clusters (Dressler *et al.* 1999; Poggianti *et al.* 1999). However, also notable is the presence of a well developed population of 'old' stellar systems as a substantial fraction of the luminous ellipticals that dominate clusters today seem to be well in place by z∼0.4.

The unique HST imaging capabilities at *ultraviolet* wavelengths allow us now to complement the above observations by exploring for the first time the *rest-frame*, far- and mid-UV portion of galaxy SEDs in this rich cluster. The importance of such data can be appreciated taking into account that mid-UV colors provide tighter constraints to the evolution in time and composition of aging stellar populations than optical-band indices do (cfr. Dorman & O'Connell 1997). What is more, the far-UV region (and – at a lower level – the mid-UV itself) represent direct probes of star-formation activity and – through the UV-upturn phenomenon – an additional clue to the composition and age of old populations. The relative intensity of the far-UV flux changes rapidly both for young *and* old stellar systems indeed, according either to the fast evolution of recently formed UV-bright stars or the sudden onset of hot *evolved* components like those observed in present-day stellar populations of elliptical galaxies.

The very limited access to the UV imaging in the past years heavily hampered this kind of studies, however. The very few papers available in the literature make use of the datasets provided by the FOCA balloon-borne Telescope (Donas *et al.* 1995, 1997) and the Ultraviolet Imaging Telescope (UIT) during the Astro-1, Astro-2 missions onboard Space Shuttle (Cornett *et al.* 1998). These analyses could not be extended to clusters farther than z=0.23, while the approach recently adopted by Brown *et al.* (1998) to get deep HST data of the ellipticals in the cluster Abell 370 at z=0.375 is in turn hampered by the small size of the FOC field.

B.2 Observations And Reductions

Ultraviolet images of CL0939+4713 were obtained with the WFPC2 on January, 14-15, 1996 (Proposal ID: 5919). A total of five orbits (2800 s exposure time each) were spent through the filter F300W (restframe mid-UV $\lambda \sim 2000$ Å), while ten additional orbits (again 2800 s exposure time) were devoted to observations through the less sensitive filter F218W (restframe far-UV $\lambda \sim 1500$ Å). The adopted WFPC2 field was approximately the same as that chosen for the pre-existing, optical F702W images of the cluster (cfr. Dressler *et al.* 1994b). Our UV images and newly in-flight calibrated, dearchived optical frames were separately aligned, co-added and properly cleaned from cosmic ray signatures. After separately subtracting a constant sky level to each WFPC2 chip (this is made possible also for F702W frames by the higher quality flat-fielding of the data provided by the current pipeline), we performed aperture photometry on the F300W, F218W and F702W final images. Standard HST magnitudes (STMAG) m_{300}, m_{702} of each obvious source identified in our UV F300W image have been derived, together with m_{218} magnitudes for the two sources identifiable at shorter wavelengths (the flux, within the adopted aperture of $0\farcs6$ in radius, is at least 5σ above the noise, for all chosen sources). Such an aperture gives the lowest scatter in our derived magnitudes and represents a good compromise between the need of picking up as much signal as possible and

Table B.1: Abell851 F218W Photometry.

ID	S97 Number	X	Y	m_{218}	$m_{218} - m_{300}$	$m_{218} - m_{702}$	T-Type
(1)	(2)	(3)	(4)	(5)	(6)	(7)	(8)
32	497	139	768	20.66	-0.56	-1.62	4
60	230	734	458	20.44	-0.45	-1.63	10

Notes—Col. (1): Object identifier; Col. (2): Cross identification of objects against the catalog in Smail et al. (1997); Col. (3): X centroid on the mosaicked F300W frame in pixels; Col. (4): Y centroid on the mosaicked F300W frame in pixels; Col. (5): 1.″2 diameter aperture magnitude (STMAG) measured in the F218W waveband; Col. (6): Color in a 1 .″2 diameter aperture (m_{300} magnitude being measured in the F300W waveband); Col. (7): Color in a 1.″2 diameter aperture (m_{702} magnitude being measured in the F702W waveband); Col. (8): Standard T-Type.

avoiding the danger of including more than one object. All UV/optical colors used later in our CMDs refer to the above aperture.

B.3 Results

For each object detected in the near-UV final image F300W (sixty out of the 181 classified in the optical by Dressler *et al.* 1994b) we provide in Table B.2 our measured UV STMAG m_{300}, together with the UV/optical color ($m_{300} - m_{702}$). Analogously, for the two F218W detected galaxies one can derive a STMAG m_{218}, both colors ($m_{218} - m_{300}$) and ($m_{218} - m_{702}$) are provided in Table B.1.

Near-UV and optical WFPC2 images are shown in Fig. B.1 and Fig. B.2, respectively. The smaller PC1 field has been excluded from our analysis, due to the lower signal-to-noise it provides. Observed bright objects in the restframe mid-UV (F300W; $\lambda \sim 2000$ Å) are typically spiral galaxies (often with the majority of the UV flux coming from ultra-luminous sites of star formation along spiral arms) as well as a few irregular and/or merging systems, while the optically most prominent giant ellipticals virtually disappear at UV wavelengths. However, one should be put on his guard against believing that the totality of spirals identified by HST in the optical can be easily detected in the mid-UV (F300W) waveband. The majority of such objects escape detection, instead. Their weak UV appearance, besides being borne out by the large fraction of Sa, Sb spirals showing optically passive energy distributions (k and k+a classes of Dressler *et al.* 1999) in intermediate-redshift clusters, could be related to the enhanced role of internal extinction in the UV.

The overall HST c-m diagram (m_{702} *vs.* $m_{300} - m_{702}$) of the sources detected at UV wavelengths is given in Fig. B.3. Here the ($m_{300} - m_{702}$) color derived from our aperture photometry (0.″6 radius) is compared with *integrated* m_{702} magnitudes given by Smail *et al.* (1997). The reason is the latter magnitudes are representative of the *total* optical flux of the galaxies, whereas our aperture photometry, though well-suited to give reliable (UV−Optical) colors, is not. Specific diagrams within the same figure isolate galaxies for which – on the basis of the spectroscopic and spectrophotometric redshifts provided by Dressler *et al.* (1999) and Belloni and Röser (1996) – one can *firmly establish the association* either with CL0939 +4713 or the projected field, respectively. As far as the membership to CL0939+4713 is concerned,

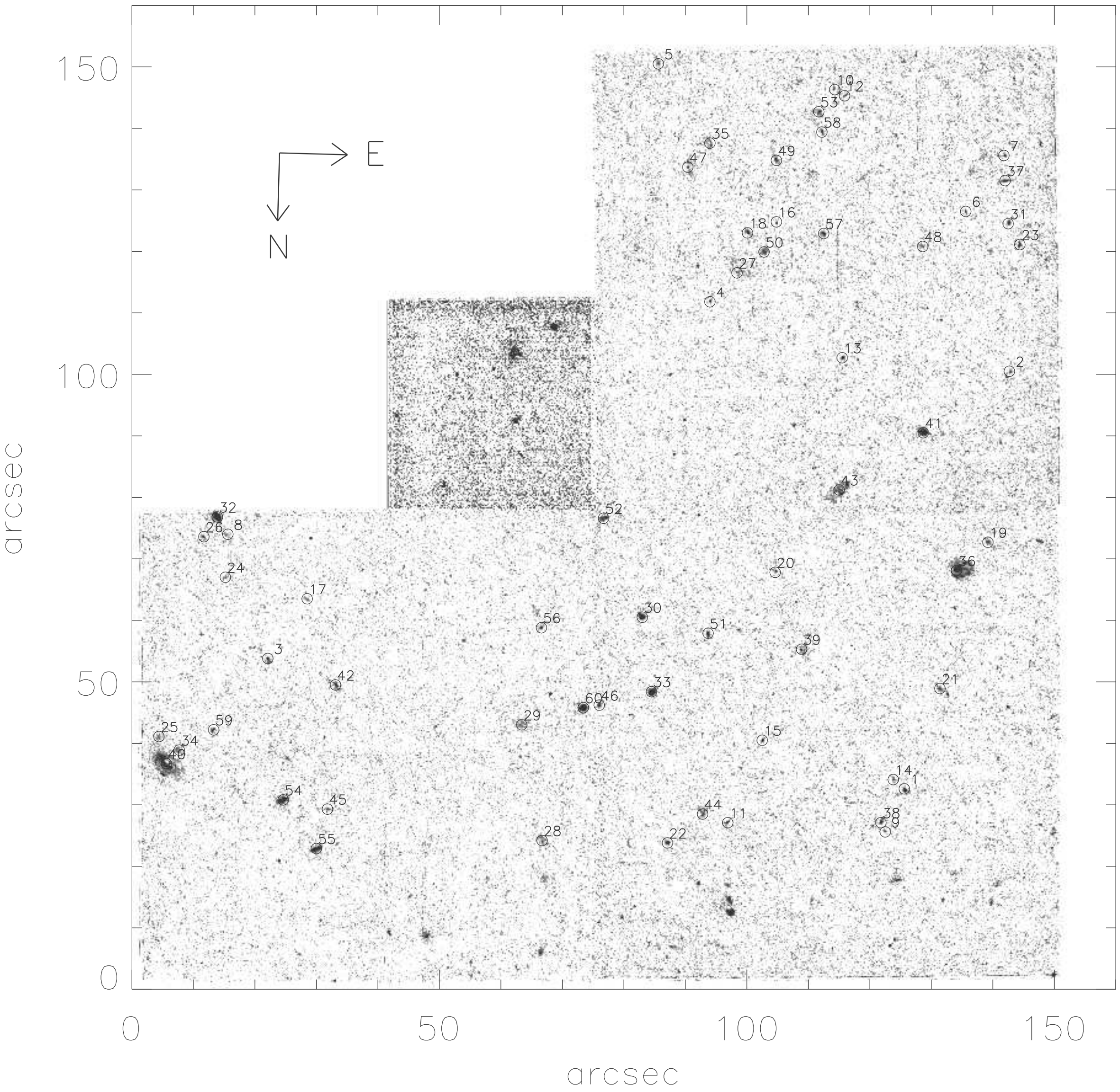

Figure B.1: Five-orbit, co-added near-UV WFPC2 frame of CL0939+4713 (imaged through the F300W filter). A logarithmic display scale has been adopted. Detected galaxies are marked with a circle and the sequence number adopted in Table 1 and 2. Note that galaxies identified as source no. 32 and no. 60, respectively are the only objects detected also in mid-UV (F218W) frames. The PC1 field has been excluded from our analysis, due to its higher noise.

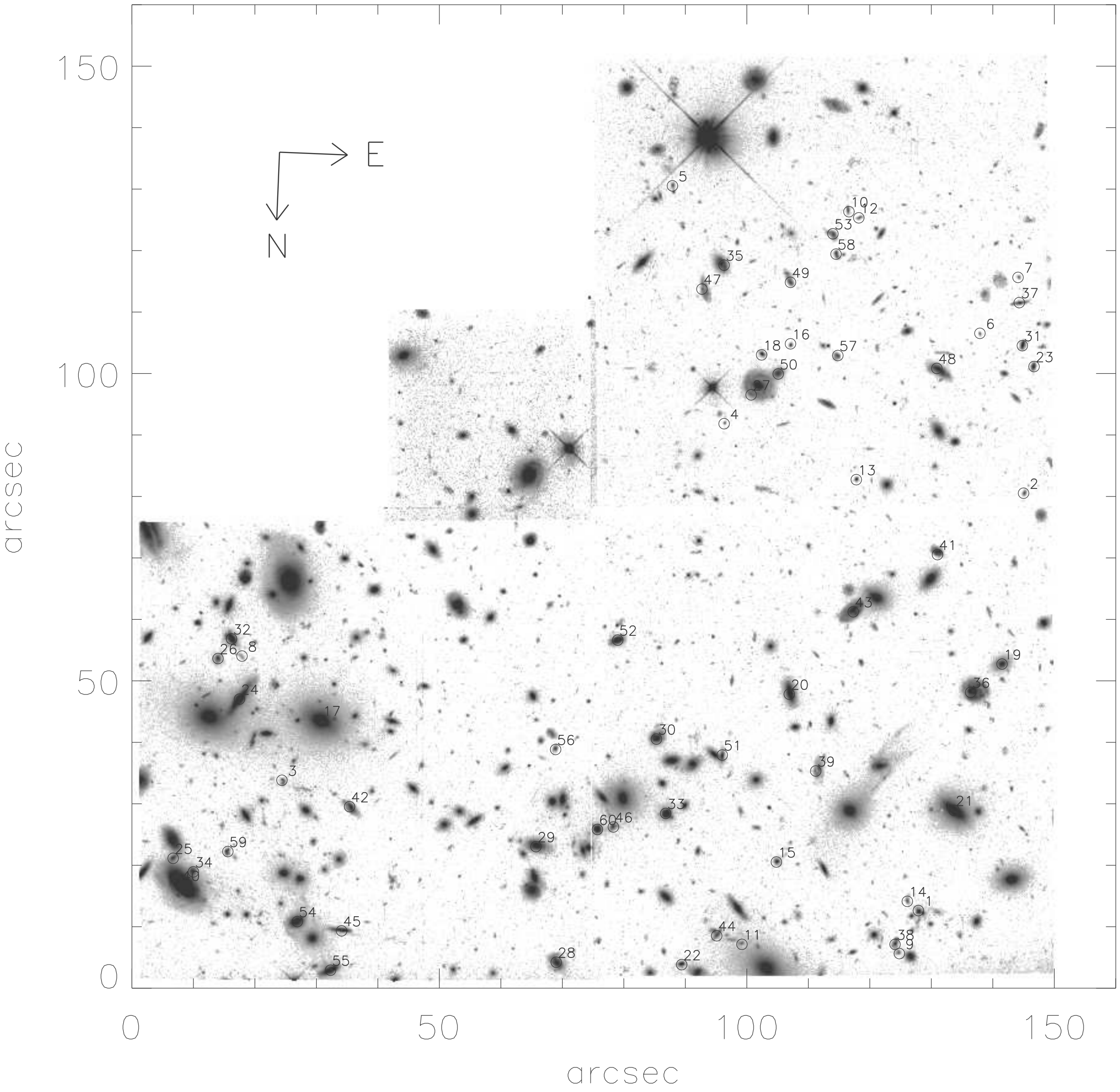

Figure B.2: Comparison optical (F702W) WFPC2 frame of CL0939+4713. Again, a logarithmic display scale has been adopted. Sources detected in the F300W waveband are marked as in previous figure for cross-identifying purposes. The fields of optical and UV images do not match perfectly, being shifted of ∼20 arcsec approximately along the North-South direction.

Table B.2: Abell851 F300W Photometry

ID (1)	S97 Number (2)	X (3)	Y (4)	m_{300} (5)	$m_{300} - m_{702}$ (6)	T-Type (7)
1	125	1256	326	21.53	-0.81	-99
2	660	1427	1005	23.76	-0.99	-99
3	301	221	538	23.33	-1.15	-99
4	706	940	1118	23.59	-2.01	-99
5	892	856	1505	23.63	-1.18	-99
6	768	1356	1265	24.11	-1.78	-99
7	805	1418	1356	23.78	-1.77	-99
8	457	156	740	24.03	-1.40	-99
9	64	1225	256	24.61	-0.38	-99
10	873	1143	1463	23.85	-0.71	-99
11	72	969	271	23.34	-1.39	-99
12	866	1159	1453	24.02	-0.91	-99
13	674	1155	1027	22.97	-1.35	-99
14	136	1238	341	23.78	-0.95	-99
15	178	1025	405	23.23	-0.21	-99
16	760	1048	1248	24.07	-0.66	-99
17	399	285	635	23.92	3.31	-5
18	752	1001	1230	22.60	-1.02	-4
19	455	1392	727	23.22	0.46	-3
20	425	1046	678	23.80	2.89	-2
21	273	1314	489	23.27	3.05	-2
22	35	871	238	22.60	-0.60	-2
23	738	1444	1211	22.92	-0.40	1
24	427	152	670	23.88	3.37	1
25	3017	44	411	23.53	0.01	1
26	456	117	736	23.51	-0.07	2
27	735	984	1165	23.58	-0.26	3
28	43	667	242	23.37	0.81	4
29	215	634	430	23.29	1.26	4
30	369	830	605	21.79	-0.34	4
31	763	1425	1245	23.09	0.19	4
32	497	139	768	20.66	-1.06	4
33	258	845	484	21.52	0.05	4
34	3006	77	389	23.29	0.15	5
35	824	940	1376	23.58	0.51	5
36	422	1341	681	21.91	-0.30	5
37	788	1420	1315	23.16	-0.79	5
38	65	1218	271	23.15	-0.65	5
39	321	1089	553	23.30	-0.82	6
40	224	56	367	23.03	1.96	6
41	601	1287	905	21.65	-1.23	6
42	261	331	495	22.75	-0.24	6

Table B.2: Abell851 F300W Photometry

ID	S97 Number	X	Y	m_{300}	$m_{300} - m_{702}$	T-Type
(1)	(2)	(3)	(4)	(5)	(6)	(7)
43	540	1150	812	23.28	0.82	6
44	84	928	285	23.24	-0.58	6
45	123	318	293	23.87	1.17	6
46	232	760	462	23.07	-0.68	6
47	806	904	1337	23.84	-0.48	7
48	742	1286	1208	23.86	1.24	7
49	809	1048	1348	23.18	-0.74	7
50	736	1028	1199	22.91	-0.29	7
51	339	937	579	23.05	-0.47	7
52	489	767	766	22.61	0.33	7
53	851	1117	1427	23.19	-0.74	7
54	122	246	308	21.86	0.30	7
55	36	300	229	21.69	0.26	7
56	342	666	588	23.49	-0.82	10
57	750	1125	1229	22.91	-1.29	10
58	829	1122	1394	23.40	-0.60	10
59	191	133	422	23.29	-0.43	10
60	230	734	458	20.44	-1.18	10

Notes—Col. (1): Object identifier; Col. (2): Cross identification of objects against the catalog in Smail et al. (1997); Col. (3): X centroid on the mosaicked F300W frame in pixels; Col. (4): Y centroid on the mosaicked F300W frame in pixels; Col. (5): $1''\!.2$ diameter aperture magnitude (STMAG) measured in the F300W waveband; Col. (6): Color in a $1''\!.2$ diameter aperture (m_{702} magnitude being measured in the F702W waveband); Col. (7): Standard T-Type; an undefined entry is given as -99.

a conservative criterion, namely Δz=0.39–0.42, essentially matching that of Dressler *et al.*, has been adopted.

By cross-identifying our UV sources and the galaxies optically classified within the same WFPC2 field by Smail *et al.* (1997) one can ascribe a broad morphological classification (namely, E/SO, Spiral or Irregular) to the majority of objects detected in our F300W image. This, in turn, allows us to draw some basic conclusions about the appearance of these UV-bright members of each class. While spirals clearly span quite a large range in optical luminosity *and* UV/optical color ($\approx$ 5 mag in both m_{702} and $[m_{300} - m_{702}]$ color), bright (m_{702} <22) early-type galaxies are always fairly red ($[m_{300} - m_{702}] \sim 3$) and detectable irregular galaxies are constantly bluer than $(m_{300} - m_{702}) = 0$. As far as this behavior is concerned, no significant differences emerge when comparing confirmed cluster and field galaxies.

A separate issue is represented by fainter, *particularly UV-bright* compact sources falling in the lower left region of the diagram and whose morphology cannot be reliably identified. These objects presumably represent quite a heterogeneous zoo, including individual clumps of vigorous star formation within amorphous, low-luminosity galaxies and mergers belonging

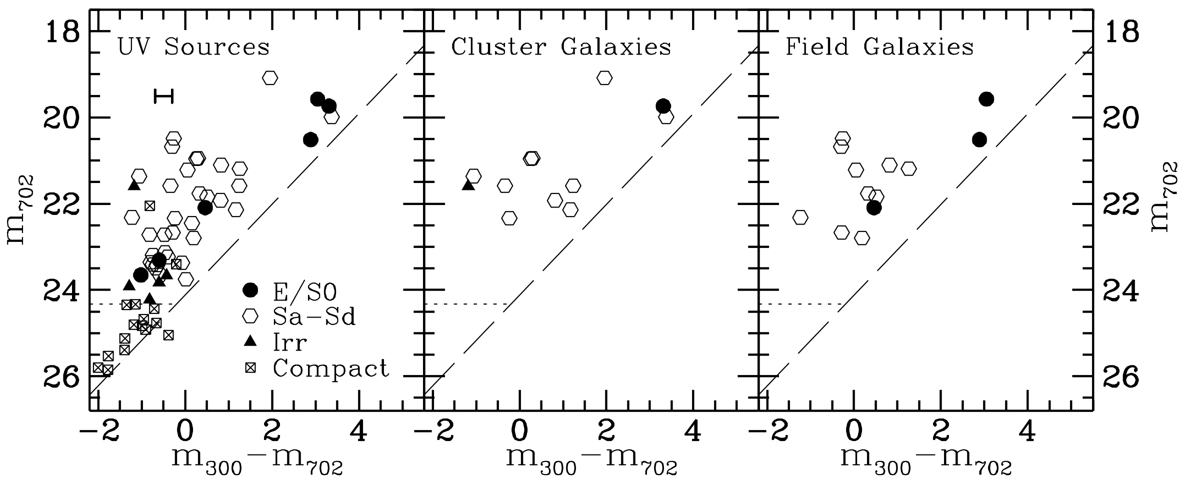

Figure B.3: *Left Panel:* Overall c-m (m_{702} *vs.* $[m_{300} - m_{702}]$) diagram of the sources detected in the WFPC2 frames centered on CL0939+4713. The ($m_{300} - m_{702}$) color derived from our aperture photometry ($0.6''$ radius) is compared with *integrated* m_{702} magnitudes given by Smail *et al.* (1997) after applying a zeropoint correction of 0.85 mag to take properly into account the value of the detector gain. A key to the morphological types is inserted. Shaded line and dotted line represent the detection limit imposed by our UV images and the limit magnitude adopted by Smail *et al.* for their (optical) morphological classification, respectively. Formal errors of our HST UV photometry are shown by the representative error bar. Formal errors for HST optical measurements are negligible. *Central Panel:* the same for spectroscopically confirmed members of CL0939+4713 alone. *Right Panel:* The same for confirmed field (either foreground or background) galaxies projected onto the CL0939+4713 WFPC2 field of view.

to (or projected on) CL0939+4713, as well as background AGNs. The latter case is true for our bright source no. 1 in Table 1, identified as a background QSO at z$\sim$2 (Dressler *et al.* 1993; Hutchings & Davidge 1997).

The availability of ground-based ($g - r$) optical colors for a large fraction of objects detected in our near-UV image offers also the opportunity of constructing *two-color*, optical *vs.* UV/optical (i.e. $[g-r]$ *vs.* $[m_{300} - m_{702}]$) diagrams (see Fig. B.4). The above ($g-r$) colors come from the ground-based photometry of Dressler & Gunn (1992) and are widely discussed also in Dressler *et al.* (1994a; 1994b). HST-based and ground-based colors appear well-correlated in Fig. B.4, in such a way that, *a posteriori*, one can assume ($g-r$) colors are highly predictive of the $m_{300} - m_{702}$ colors of galaxies, too. Moreover, no evidence of a dichotomy between spirals experiencing steady-state star-formation and possible, UV-dominated spirals undergoing major starbursts is seen.

B.4 Comparison with a Present-Day Cluster Population

As stressed above, the restframe mid-UV region – besides its higher sensitivity to the effect of age and metal content of *old* populations when compared to the optical – is quite sensitive to the presence of some amount of *young* stars, too (cfr. Burstein *et al.* 1988). As a consequence, our newly obtained UV data provide a direct tool to investigate the present and past role

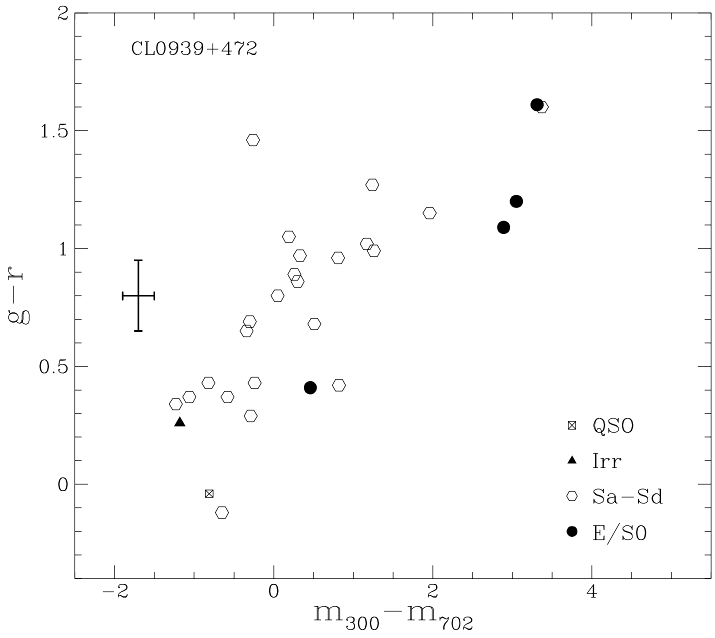

Figure B.4: Two-color, ($[g - r]$ *vs.* $[m_{300} - m_{702}]$) diagram of all sources simultaneously detected in the UV within the CL0939+4713 WFPC2 field and photometered from ground by Dressler & Gunn (1992). The ($m_{300} - m_{702}$) color always refers to an aperture of $0.6''$ in radius. A key to the morphological types is inserted. Error bars combine formal errors of our HST UV photometry and expected systematic errors of optical, ground-based photometry.

of star formation processes in cluster galaxies. This information is of paramount importance in the specific case of CL0939+4713, because – for the first time – we can push our inquiry back in time up to an intermediate-redshift cluster population of ~5 billion years ago, i.e. to some kind of "missing ring" in the current observational basis for evolutionary studies (unlike clusters at z≥2, the mid-UV region of CL0939+4713 is not accessible from ground-based observations, indeed).

For instance, the comparison with UV data of present-day galaxy clusters provide a direct way of verifying whether signs of star formation activity among member galaxies persist at the same/higher/lower level when looking back at z~0.4 (at least as far as the two galaxy samples are comparable). Moreover, when compared with suitable models of populations (either purely old or hosting some recent star formation), our data allow us to establish how recently UV-bright galaxies detected by WFPC2 underwent their last episode of star formation. In the following, analyses like those sketched above are applied to our F300W photometry of CL0939+4713.

In particular, the availability of balloon-borne, mid-UV images of the nearby Coma cluster obtained by Donas *et al.* (1995) make it obligatory (though tricky, as discussed below) to compare these data with our HST magnitudes and colors of galaxies belonging to CL0939+4713 (see Fig. B.5). By chance, the wavebands corresponding to Donas *et al.*'s UV, optical magnitudes (m_{UV}, b) match closely, when observing *local* galaxies, the wavebands imaged *at* CL0939+4713 *restframe* by our own (m_{300}, m_{702}) HST magnitudes. In other words, since we are imaging the two clusters at the same restframe wavelengths, we are allowed to compare their populations taking into account the relative distance modulus and a zeropoint

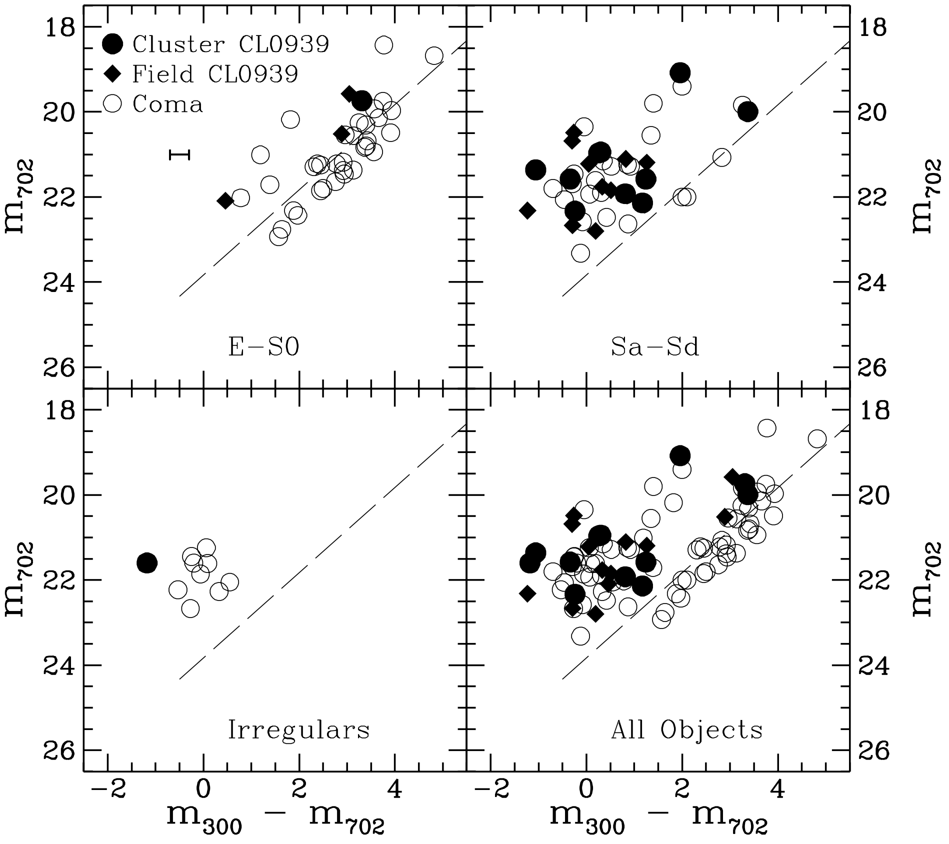

Figure B.5: UV/optical c-m diagrams superimposing CL0939+4713 member galaxies (filled circles), CL0939+4713 field galaxies (filled diamonds) and Coma cluster galaxies (open circles), splitted into morphological classes. A relative distance modulus $\Delta\mu$=6.47 is assumed to scale down UV/optical magnitudes (m_{UV}, b) of Donas *et al.* for Coma to our observed HST magnitudes (m_{300}, m_{702}). A further correction of 0.65 mag has been added to b magnitudes to remove the zeropoint mismatch between the two photometric systems. Only UV-bright galaxies for which an optical morphological classification is available are included. The shaded line represents the detection limit of WFPC2 observations. Formal errors of our HST UV photometry are shown by the representative error bar. Formal errors for HST optical measurements are negligible.

shift between HST and Donas *et al.*'s photometry alone (i.e. without applying the usual K-correction). Unlike the preliminary, similar figure shown by Buson *et al.* (1998), field galaxies are now made distinguishable from those belonging to CL0939+4713, while objects lacking a redshift estimate have been removed.

Actually, when comparing the UV properties of the two populations superimposed in Fig. B.5 and spaced in redshift by an amount Δz$\sim$0.4, one should be fully aware of the heavy observational biases and limitations involved.

First, the FOCA aperture used to image the nearby Coma cluster consists of a circular aperture of about 1° in radius, while the three WF CCDs of the WFPC2 camera cover a field of $75'' \times 75''$ each. Even normalizing to the same angular diameter distance, it turns out that the UV data of Coma come from a FOV 18× larger, whose radius exceeds by many times the cluster (X-ray) core radius (Briel *et al.* 1992); conversely, our HST images of CL0939+4713 cover a region well within the cluster core radius ($r_c \sim 3'$; Schindler & Wambsganss 1996). Secondly, despite a large observational effort, the number of redshift measurements for alleged members of CL0939+4713 is still confined to a few tens (Dressler *et al.* 1999), thus implying that the number of UV-bright galaxies detected within the WFPC2 field (60 altogether) which can be assigned either to the cluster or the field population by means of a reliable redshift estimate is necessarily tiny, as yet. Finally, when seen at CL0939+4713 redshift, a significant fraction of a hypothetical galaxy population with UV properties identical to those of Coma cluster ellipticals would fall beyond the detection limit of the WFPC2 observations presented here, being too red (see Fig. B.5). This is confirmed by the very low detection rate of early-type systems at z=0.4, as all 13 but one E/S0s within the WFPC2 field listed as CL0939+4713 members by Dressler *et al.* (1999) escape detection in the UV.

As a consequence, the remarkably different portion of cluster population sampled by the two kinds of UV experiments, together with the poor absolute statistics of suitable cluster/field WFPC2 detections, prevent us from drawing any significant conclusion about possible large-scale population differences between CL0939+4713 and Coma in the UV. The same is obviously true when comparing CL0939+4713 and its own field. At this stage one can simply notice that c-m diagrams of Fig. B.5 do not offer any evidence in favor of the presence – among the *centrally-located* galaxy population of CL0939+4713 – of objects much bluer (i.e. UV-brighter) than the bluest star-forming galaxies pervading the present-day Coma cluster. This, in turn, suggests that the excess of star-forming objects noticed at z$\sim$0.4 does not imply an enhanced star-formation rate in *individual* galaxies. However, we want to stress once more that the possibility of quantifying the role of a large-scale phenomenon such as the Butcher-Oemler effect in the mid-UV is beyond the capabilities of the WFPC2 UV data of CL0939+4713 discussed here.

B.5 Comparison with Evolutionary Models

As already pointed out, one can complement the above analysis by comparing the location within UV/optical c-m diagrams of our detected galaxies with that of suitable population models. In this way one can estimate how frequently individual cluster galaxies are affected by major episodes of intervening star formation (up to continuous star formation processes, obviously indistinguishable from a very recent event). In the following we restrict our analysis to spheroidal galaxies alone, i.e. avoiding young-population dominated spiral and/or irregular galaxies. Owing to the lack of an actively star-forming disk, ellipticals are indeed the best tracers of phenomena capable of triggering *episodic* star formation in clusters, such as merging and/or tidal disturbances, intergalactic gas stripping and ram pressure and so on.

Such a comparison is shown in Fig. B.6, where model spheroidal galaxies representing passively evolving populations with/without the addition of some amount of younger stars of different age are superimposed to our mid-UV/optical c-m diagram for elliptical galaxies belonging to CL0939+4713, its own field, and Coma (as seen at z=0.41), respectively. More precisely, models on the right side of the figure represent aging single-burst populations at a fixed age of 10.8 Gyr (the estimated age of CL0939+4713 when adopting H_0=50 km s^{-1} Mpc^{-1}, q_0=0 and z_f=5). Only two representative galaxy masses (10^{10} $M_\odot$ and 10^{12} $M_\odot$, respectively) are shown here; a characteristic time τ corresponding to 0.1$\times$ the Hubble time has been adopted for the initial starburst. When recent episodes of star formation are added to

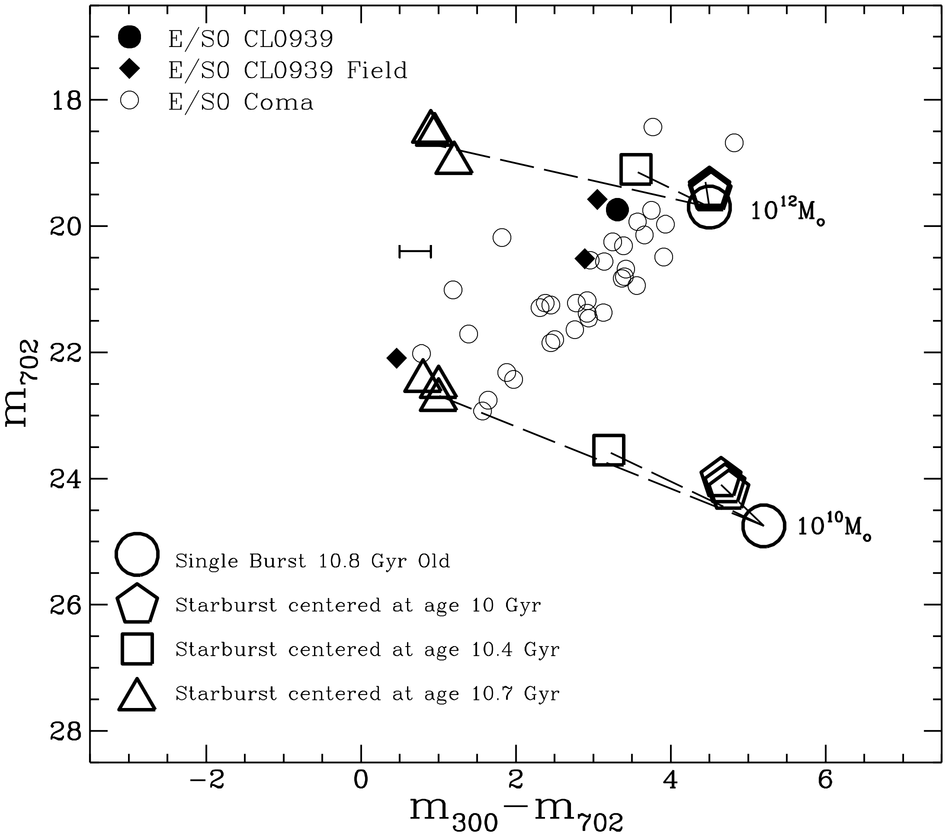

Figure B.6: Models showing the expected location of both passively evolved and young-population contaminated ellipticals, superimposed to the UV/ optical c-m diagram for early-type galaxies of both CL0939+4713 and Coma clusters. Both models and galaxy magnitudes have been scaled to z=0.41. The meaning of symbols, both for data and models, is given by the key in figure. On the right side are represented galaxies at a fixed age of 10.8 Gyr with mass of 10^{10} $M_\odot$ and 10^{12} $M_\odot$, respectively, which consist of an aging, uncontaminated single-burst population. Dashed lines connect these passive models to their expected location in case they have experienced recent 'rectangular' bursts having constant duration (10^8 yr) and slightly different efficiencies ν_b (within 1-3%), centered at a time τ_b of 0.1, 0.4 and 0.8 Gyr before the epoch recorded by our observations, respectively. Multiple symbols correspond to the above slightly different efficiencies of the recent burst. Formal errors of our HST UV photometry are shown by the representative error bar. Formal errors for HST optical measurements are negligible.

the above models the representative points of such "contaminated" populations move towards the left (blue) portion of the CMD. In particular, our computations show the effect of adding to the model ellipticals recent 'rectangular' bursts with slightly different efficiencies ν_b (within 1-3%) and constant duration (10^8 yr), centered at a time τ_b of 0.1, 0.4 and 0.8 Gyr before the epoch recorded by our observations respectively.

One can recognize two major features when comparing UV observations and models:

1. Passively evolved populations fall beyond the detection capabilities of the UV observations discussed here and—what is more—secondary bursts experienced by galaxies

earlier than 0.8 Gyr before the observing epoch are fully reabsorbed in terms of restframe mid-UV/optical colors, independently of galaxy mass and luminosity; this implies that *all spheroidal galaxies UV-bright enough to be detected in our HST F300W (as well as balloon-borne) images did host a starburst in the near past (typically 100-300 Myr earlier) or, alternatively, undergo a low-level, continuous star formation activity.*

2. Among the numerous UV-bright, early-type galaxies seen in Coma (and not at the center of CL0939+4713), signs of very recent (and thus presumably frequent) star formation activity is shown preferentially by low-luminosity objects. In this respect, it is worth mentioning that the existence of this kind of continuous rejuvenation for Coma cluster low-luminosity early-type galaxies (i.e. a series of overlapping short bursts) is largely supported also by recent spectroscopic observations (Caldwell & Rose 1998) showing that a significant fraction of these faint members do host a young population superposed to older stars.

B.6 Looking at CL0939+4713 in the Far-UV

As already pointed out, our HST observations aimed also at exploring the far-UV portion of the *restframe* energy distribution of galaxies at z$\sim$0.4. Actually, the presence of a far-UV excess (upturn) in metal-rich, evolved populations is known since the early epochs of UV space astronomy (Code 1969; Code & Welch 1979; Bertola *et al.* 1980, 1982, 1986; Oke *et al.* 1981) and *the goal of recording its onset and subsequent evolution at intermediate redshift is still a major observational challenge* (see Greggio & Renzini 1999 and O'Connell 1999 for comprehensive, recent reviews).

In particular, on the basis of current galaxy evolutionary models (e.g. Bressan *et al.* 1994; Tantalo *et al.* 1996), one should expect that – owing to the vanishing of post-HB evolutionary paths (Post Early-AGB stars, AGB-Manqué stars) which generate most of the present-day UV-bright stars – the UV properties of old populations in giant ellipticals do show a dramatic change, when observed to a proper lookback time (which could well fall around CL0939+4713 redshift). In other words, looking back in time a few billion years, one should witness some kind of 'switching off' of the UV-upturn seen in present-day giant ellipticals, thus recording restframe 1550$-$V colors much redder than their present value.

Unfortunately, the restframe far-UV emission (F218W) of almost the totality of galaxies detected in the restframe mid-UV (F300W) could not be recorded and even the upper limits to the level of the far-UV flux in individual ellipticals at z=0.4 implied by our WFPC2 observations are too high to provide the sought astrophysical constraints. More precisely, the upper limit to the UV emission imposed by adding F218W counts in the *total* frame area occupied by the *whole sample* of optically-bright ellipticals in the corresponding F702W frames, implies that one cannot detect objects (at 3 σ limit) whose restframe UV/optical color is higher (i.e. *redder*) than (1550–V)=1.0. Such a (blue) color can be reached among present-day galaxies only by actively star-forming systems, while even the nearby UV-brightest old populations in ellipticals are not bluer than (1550–V)$\sim$2 and, as such, could not be detected (*cfr.* Burstein *et al.* 1988).

As a consequence, the set of (F218W) UV data discussed here are inadequate to establish the existence and amplitude of the UV-upturn phenomenon typical of present-day evolved populations at CL0939+4713 lookback time. This outcome is consistent with similar unconclusive results reached by other groups who observed clusters at similar distance with the same instrumental configuration (e.g. Renzini 1996). This conclusion – though negative – does not imply that such a kind of investigation is *strictly* beyond HST capabilities, however, and is presently pushing other groups to explore alternative observing approaches. In this respect, the very recent positive result of Brown *et al.* (1998) – who were able to sample the UV-upturn of *a few* ellipticals belonging to a cluster of similar redshift (Abell 370; z=0.375) by combining two FOC long-pass filters – holds the hope of exploiting successfully HST in the near future, in particularly with the planned installation of the Advanced Camera for Surveys (ACS).

B.7 Conclusions

This work can be considered as the first "journey" into the restframe UV of an *intermediate-redshift*, rich galaxy cluster. Making use of HST, we were able to detect in a single WFPC2 field tens of UV-bright sources belonging either to CL0939+4713 or to its close foreground or background. Newly obtained UV data have been combined with pre-existing HST and ground-based optical images to derive unprecedented UV/Optical c-m and two-color diagrams. While irregular and (luminous) early-type galaxies are well-confined to specific color ranges within such diagrams, spirals do exhibit quite a large variability in color.

In order to explore possible evolutionary effects, HST data of CL0939+4713 have been finally compared with balloon-borne UV data of the *local* Coma cluster. Although an *exhaustive* comparison of the hottest populations of nearby and intermediate-redshift clusters has to wait until deeper, wide-field UV surveys of distant clusters will become available, the limited datasets discussed here do provide interesting pieces of evolutionary information. For instance no hints of a fast evolution in the UV from z$\sim$0.4 to present time (in the sense of cluster galaxies at z$\sim$0.4 hosting a star-formation activity dramatically higher than their present-day counterparts) are found.

Bibliography

Andreon, S., Davoust, E., & Heim, T. 1997, A&A, 323, 337

Belloni, P., Bruzual, A.G., Thimm, G.J., & Röser, H.-J. 1995, A&A, 297, 61

Belloni, P., & Röser, H.-J. 1996, A&AS, 118, 65

Bertola, F., Capaccioli, M., Holm, A.V., & Oke, J.B. 1980, ApJ, 237, 65

Bertola, F., Capaccioli, M., & Oke, J.B. 1982, ApJ, 254, 494

Bertola, F., Gregg, M. D., Gunn, J. E., & Oemler, A., Jr. 1986, ApJ, 303, 624

Bressan, A, Chiosi, C., & Fagotto, F. 1994, ApJS, 94, 63

Briel, U.G., Henry, J.P., & Böhringer, H. 1992, A&A, 259, L31

Brown, T.M., Ferguson, H.C., Deharveng, J.-M., & Jedrzejewski, R.I. 1998, ApJ, 508, 139

Burstein, D., Bertola, F., Buson, L.M., Faber, S.M., & Lauer, R.L. 1988, ApJ, 328, 440

Buson, L.M., Bertola, F., Cappellari, M., Chiosi, C., Dressler, A. & Oemler, A. 1998, in ASP Conf. Proc. 146, The Young Universe: Galaxy Formation and Evolution at Intermediate and High Redshift, ed. S. D'Odorico, A. Fontana & E. Giallongo, (San Francisco: ASP) 488

Butcher, H., & Oemler, A. 1978, ApJ, 219, 18

Butcher, H., & Oemler, A. 1984, ApJ, 285, 426

Caldwell, N., & Rose, J.A. 1998, AJ, 115, 1423

Code, A.D. 1969, PASP, 81, 475

Code, A.D., & Welch, G.A. 1979, ApJ, 228, 95

Cornett, R.H., Dorman, B., Smith, E.P., Fanelli, M., Oegerle, W.R., Bohlin, R.C., Neff, S.G., O'Connell, R.W., Roberts, M.S., Smith, A.M., & Stecher, T.P. 1998, ApJ, 116, 44

Couch, W.J., Ellis, R.S., Sharples, R.M., & Smail, I. 1994, ApJ, 430, 121

Couch, W. J., Barger, A. J., Smail, I., Ellis, R.S., & Sharples, R.M. 1998, ApJ, 497, 188

Donas, J., Milliard, B., & Laget, M. 1995, A&A, 303, 61

Donas, J., Viton, M., Martin, C., & Milliard, B. 1997, in The Ultraviolet Universe at Low and High Redshift: Probing the Progress of Galaxy Evolution, ed. W.H. Waller, M.N. Fanelli, J.E. Hollis, & A.C. Danks, (New York: AIP), 103

Dorman, B., & O'Connell, R.W. 1997, in The Ultraviolet Universe at Low and High Redshift: Probing the Progress of Galaxy Evolution, ed. W.H. Waller, M.N. Fanelli, J.E. Hollis, & A.C. Danks, (New York: AIP), 175

Dressler, A., & Gunn, J.E. 1983, ApJ, 290, 7

Dressler, A., & Gunn, J.E. 1992, ApJS, 78, 1

Dressler, A., Oemler, A., Gunn, J.E., & Butcher, H.R. 1993, ApJ, 404, L45

Dressler, A., Oemler, A. Jr., Butcher, H.R., & Gunn, J.E. 1994a, ApJ, 430, 107

Dressler, A., Oemler, A. Jr., Sparks, W.B., & Lucas, R.A. 1994b, ApJ, 435, L23

Dressler, A., Oemler, A. Jr., Couch, W.J., Smail, I., Ellis, R.S., Barger, A., Butcher, H.R., Poggianti, B.M., & Sharples, R.M. 1997, ApJ, 490, 577

Dressler, A., Smail, I., Poggianti, B.M., Butcher, H.R., Couch, W.J., Ellis, R.S., & Oemler, A. Jr. 1999, ApJS, 122, 51

Fukugita, M., Doi, M., Dressler, A., & Gunn, J.E. 1995, ApJ, 439, 584

Greggio, L., & Renzini, A. 1999, Mem. Soc. Astron. Italiana, 70, 691

Hutchings, J.B., & Davidge, T.J. 1997, PASP, 109, 667

O'Connell, R.W. 1999, ARA&A, preprint (astro-ph/9906068)

Oemler, A. Jr., J.R., Dressler, A. & Butcher, H.R. 1997, ApJ, 474, 561

Oke, J.B., Bertola, & F., Capaccioli, M. 1981, ApJ, 243, 453

Poggianti, B.M., Smail, I., Dressler, A., Couch, W.J., Barger, A., Butcher, H.R., Ellis, R.S., & Oemler, A. Jr. 1999, ApJ, 518, 576

Renzini, A. 1996, in Science with HST-II, P. Benvenuti *et al.*, STScI-ECF, 267

Schindler, S., & Wambsganss, J. 1996, A&A, 313, 113

Schindler, S., Belloni, P., Ikebe, Y., Hattori, M., Wambsganss, J., & Tanaka, Y. 1998, A&A, 338, 843

Seitz, C., Kneib, J.-P., Schneider P., & Seitz, S. 1996, A&A, 314, 707

Smail, I. , Dressler, A. , Couch, W. J., Ellis, R. S., Oemler, A. , Jr., Butcher, H. & Sharples, R. M. 1997, ApJS, 110, 213

Stanford, S.A., Eisenhart, P.R.M., & Dickinson, M. 1995, ApJ, 450, 512

Stanford, S.A., Eisenhart, P.R.M., & Dickinson, M. 1998, ApJ, 492, 461

Tantalo, R., Chiosi, C. Bressan, A., & Fagotto, F. 1996, A&A, 311 361

Ringraziamenti

A conclusione della stesura di questa tesi di dottorato desidero ricordare con la piú viva riconoscenza le persone che nel Dipartimento di Astronomia padovano hanno rappresentato l'intorno dello spazio entro il quale ho lavorato, e senza le quali anche gli argomenti trattati avrebbero assunto diversa configurazione.

Innanzi tutto il prof. Francesco Bertola, guida esperta e prodiga di apprezzati consigli, appassionato della ricerca astronomica e punto di riferimento per l'ambiente umano orbitante intorno a lui, che con lui studia, impara, lavora e vive.

E poi, appunto, il gruppo: Lucio Buson, Pierantonio Cinzano, Enrico Corsini, José Funes, Alessandro Pizzella, Marc Sarzi, Claudia Scarlata e Juan Carlos Vega, che, con la costruttiva vicinanza e con la disponibilitá di ognuno, ha collaborato alla conclusione di questo mio lavoro di tesi, oltre a renderlo piú piacevole e stimolante. A tutti il mio grazie cordiale, nella fiducia di averli ancora vicini sulla via della ricerca e dell'amicizia.